Author(s): Zhigalov, A.; Heinilä, Erkka; Parviainen, Tiina; Parkkonen, L.; Hyvärinen, A.

Title: Decoding attentional states for neurofeedback : Mindfulness vs. wandering thoughts

Year: 2019

Version: Accepted version (Final draft)

Please cite the original version:

Accepted Manuscript

Decoding attentional states for neurofeedback: Mindfulness vs. wandering thoughts

A. Zhigalov, E. Heinilä, T. Parviainen, L. Parkkonen, A. Hyvärinen
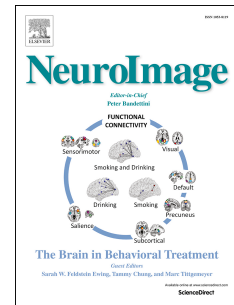
Please cite this article as: Zhigalov, A., Heinilä, E., Parviainen, T., Parkkonen, L., Hyvärinen, A., Decoding attentional states for neurofeedback: Mindfulness vs. wandering thoughts, *NeuroImage* (2018), doi: https://doi.org/10.1016/j.neuroimage.2018.10.014.

This is a PDF file of an unedited manuscript that has been accepted for publication. As a service to our customers we are providing this early version of the manuscript. The manuscript will undergo copyediting, typesetting, and review of the resulting proof before it is published in its final form. Please note that during the production process errors may be discovered which could affect the content, and all legal disclaimers that apply to the journal pertain.

1   **Decoding attentional states for neurofeedback: mindfulness vs. wandering thoughts**

2

3   Zhigalov A[1,3*], Heinilä E[2], Parviainen T[2], Parkkonen L[3], Hyvärinen A[1,4]

4

5   [1]Department of Computer Science, University of Helsinki, Finland
6   [2]Department of Psychology, University of Jyväskylä, Finland
7   [3]Department of Neuroscience and Biomedical Engineering, Aalto University, Finland
8   [4]Gatsby Computational Neuroscience Unit, University College London, UK

9

10   * Correspondence should be addressed to,
11   Alexander Zhigalov
12   Department of Neuroscience and Biomedical Engineering
13   Biomedical Engineering
14   Aalto University School of Science
15   P.O. Box 12200
16   FI-00076 AALTO
17   alexander.zhigalov@aalto.fi

18

19   **Abstract**

20   Neurofeedback requires a direct translation of neuronal brain activity to sensory input given to
21   the user or subject. However, decoding certain states, e.g., mindfulness or wandering thoughts,
22   from ongoing brain activity remains an unresolved problem.

23   In this study, we used magnetoencephalography (MEG) to acquire brain activity during
24   mindfulness meditation and thought-inducing tasks mimicking wandering thoughts. We used a
25   novel real-time feature extraction to decode the mindfulness, i.e., to discriminate it from the
26   thought-inducing tasks. The key methodological novelty of our approach is usage of MEG power
27   spectra and functional connectivity of independent components as features underlying
28   mindfulness states. Performance was measured as the classification accuracy on a separate
29   session but within the same subject.

30   We found that the spectral- and connectivity-based classification approaches allowed
31   discriminating mindfulness and thought-inducing tasks with an accuracy around 60% compared
32   to the 50% chance-level. Both classification approaches showed similar accuracy, although the
33   connectivity approach slightly outperformed the spectral one in a few cases. Detailed analysis
34   showed that the classification coefficients and the associated independent components were
35   highly individual among subjects and a straightforward transfer of the coefficients over subjects
36   provided near chance-level classification accuracy.

37   Thus, discriminating between mindfulness and wandering thoughts seems to be possible,
38   although with limited accuracy, by machine learning, especially on the subject-level. Our hope is
39   that the developed spectral- and connectivity-based decoding methods can be utilized in real-

40   time neurofeedback to decode mindfulness states from ongoing neuronal activity, and hence,
41   provide a basis for improved, individualized mindfulness training.

42

43   **Keywords**

44   **Neurofeedback, magnetoencephalography, machine learning, mindfulness**

45

46   **Introduction**

47   A brain computer interface (BCI), an essential component for neurofeedback, allows
48   translating patterns of neuronal activity in the brain to inputs or commands for external devices
49   (Wolpaw J. et al., 2002). Electroencephalography- (EEG) or magnetoencephalography-based
50   (MEG) non-invasive BCIs provide opportunities for numerous clinical, assistive and
51   entertainment applications. However, they require robust decoding of neuronal patterns: The
52   person who controls the BCI should learn to produce robust neuronal patterns and/or a device
53   that implements BCI should robustly identify these patterns.

54   Machine learning approaches have recently been successfully applied to detect some
55   cognitive operations or mental states from underlying neuronal activity (Lemm et al., 2011; Lotte
56   et al., 2007). Often, the classification is performed on the neuronal activity evoked by time-
57   locked presentation of a target stimulus or task (Blankertz et al., 2011), which maximizes the
58   signal-to-noise ratio of neuronal response. However, there are plenty of applications that require
59   detection of cognitive states from stimulus-free ongoing neuronal activity.

60   One application where machine-learning BCI could be very useful is mindfulness
61   meditation, which has been shown to have several positive behavioural outcomes (Tang et al.,
62   2014). During mindfulness meditation, attention is supposed to be focussed on the breath or a
63   similar target, but in reality, it varies over the time. Thus, it would be crucial to alert the user in
64   real-time about wandering thoughts, i.e., temporary weakening of mindfulness. Detection of
65   wandering thoughts can be considered as an example of neurofeedback system where a desired
66   mental state can be defined by the user but the corresponding brain signal is not known. Such a
67   sustained-attention neurofeedback system would presumably have many other applications, for
68   instance, in driving assistance (Schmidt et al., 2009).

69   Several functional magnetic resonance imaging (fMRI) studies suggest that activity of
70   default-mode network may underlie mind-wandering thoughts (Andrews-Hanna et al., 2014;
71   Christoff et al., 2009). On the other hand, a recent study suggests that mind wandering can be
72   represented through dynamic connectivity of the brain networks (Kucyi, 2017). Nevertheless, the
73   indirect coupling of BOLD signal with neuronal activity and the relatively low temporal
74   resolution of fMRI do not allow assessment of the contribution of short-lasting cognitive
75   processes that largely constitute wandering thoughts. Several attempts have been made to find
76   the brain correlates of wandering thoughts during sustained attention tasks with millisecond
77   resolution using electroencephalography (EEG; (Baldwin et al., 2017; Braboszcz and Delorme,

78 2011). These studies have reported changes in the power at alpha frequency during mind
79 wandering, but the neuroanatomical basis remains poorly understood because of low spatial
80 resolution of EEG. A technically more advanced, simultaneous EEG-fMRI neurofeedback study
81 (Ros et al., 2013) showed an increase of connectivity in default-mode network, which was
82 positively correlated with changes in mind-wandering as well as resting state alpha rhythm.
83 Although this study provided a link between the brain rhythms and anatomy for mind-wandering,
84 the relationship between EEG and BOLD signal is rather indirect (Scheeringa et al., 2011).
85 Surprisingly, there is a lack of magnetoencephalography (MEG) studies. MEG provides better
86 temporal resolution compared to fMRI and better spatial resolution compared to EEG, which
87 allow assessing fast neuronal processes and brain networks that are closely related to fMRI
88 networks (Brookes et al., 2011).

89 In this study, we designed a behavioural paradigm where the subject performed
90 mindfulness meditation, and two different tasks mimicking wandering thoughts, in consequent
91 blocks. In contrast to mindfulness meditation, the latter tasks supposedly induced numerous
92 thoughts, e.g., related to positive future plans or anxious emotional scenes. We used active tasks
93 instead of resting state as a contrast for mindfulness meditation, because variability of resting
94 state activity seems to be too unspecific, possibly related to various preceding mental states,
95 including mindfulness itself. We developed and applied spectral- and connectivity-based
96 classification approaches to discriminate the behavioural states based on their underlying
97 neuronal activity, in particular focussing on the choice of feature extraction methods.

98 Our results show that it is possible, to some extent, to detect wandering thoughts in on-
99 going MEG measurements, and we provide a sketch of a pipeline for optimizing such detection.
100 Furthermore, in addition to the conventional view that mindfulness meditation is characterized
101 by changes in the power of alpha oscillations, the changes in (dynamic) functional connectivity
102 may provide an alternative, possibly even better, description of mindfulness states.

103

104 **Materials and Methods**

105 *Experimental design*

106 Twenty-four subjects (9 females, 27±5.5 years (mean±SD)) with moderate or no previous
107 experience in mindfulness meditation participated in the study. Prior to the study, we performed
108 a screening to include subjects with no history of neurological disorders, head trauma or
109 substance abuse. All participants had normal or corrected to normal vision. Ten subjects had no
110 previous experience, while other subjects had experience in either focused attention or open
111 monitoring meditation practices ranged from 0.5 to 10 years.

112 After a 2-minute resting state, participants were instructed to perform one of the tasks while
113 undergoing MEG (Elekta Neuromag, TRIUX). The tasks were organized into 2-minute blocks
114 with counterbalanced order and the participants performed each task four times in a single
115 session. The session ended with a resting state 2-minutes block. We conducted two sessions per
116 participant with a 5-minutes break between the sessions (Fig. 1).

117   -------------------------------

118   **Figure 1 about here**

119   -------------------------------

120 Fig. 1. Diagram of the experiment. The tasks are MF (mindfulness meditation), FP (reflection of
121 future planning) and EP (reflection on anxiousness-inducing emotional pictures).

122 The tasks were mindfulness meditation (MF), reflection on future planning (FP) and reflection
123 on anxiousness-inducing emotional pictures (EP). In all tasks, subjects were instructed to sit still,
124 fix the gaze on the crosshair, and perform a task after a short (seven seconds) visual instruction.
125 The visual instruction was shown at the beginning and at the middle of each task (Fig. 1) to keep
126 subjects' attention. After each task, the subject was asked to evaluate his/her involvement in the
127 task by answering two questions "How focussed were you on the task?" and "How did you feel
128 during the task? (pleasantness)" using a touch pad that provided a gradual response within range
129 from 0 to 1.

130 For the *mindfulness meditation task*, the subject was instructed to focus his/her attention on the
131 sensations of breathing and move his/her focus of attention back to the task if mind-wandering
132 occurs. The task started with a visual instruction "Please focus on your breathing" accompanied
133 by a picture of clouds. For the future planning and anxiety-inducing tasks, the subject
134 individually selected 16 (out of 40) relevant pictures prior to the experiment. In the *future
135 planning task*, subject was asked to perform a planning related to the picture, presumably
136 following the ensuing chains of thought and keeping his/her mind busy. The task started with an
137 instruction "Please make plans related to the picture" accompanied by a relevant picture. The
138 *anxiety-inducing task* was similar to the future planning, but instead of neutral pictures,
139 disturbing, scary, disgusting or other unpleasant pictures were shown to the subject. The task
140 started with a visual instruction "Place yourself or someone close to you in this situation"
141 accompanied by a relevant picture. For the FP and EP tasks two different pictures were presented
142 for each 2-minute block (at the beginning and in the middle), and for the MF task, the same
143 picture of clouds was presented twice.

144 *Analysis of behavioural data*

145 We analysed the subject's responses for the question "How focussed were you on the task?" (see,
146 Fig. 1) ranged from 0 to 1. The average values were the following 0.65 ± 0.012 (mindfulness),
147 0.70 ± 0.010 (future planning task) and 0.66 ± 0.013 (anxiety-inducing task) respectively. This
148 result showed that the focus during different tasks was at a reasonable level. Additionally, we
149 compared the responses between different tasks using the Wilcoxon rank sum test. The results
150 showed no significant difference ($p > 0.05$) between the tasks, suggesting that the participants
151 performed these tasks equally well.

152 *Data pre-processing*

153 In the analysis, we used the 204 planar gradiometers of the MEG scanner. The Signal Space
154 Separation (SSS) method (Taulu et al., 2004) was applied to supress the external interference and
155 sensor artefacts.

Independent component analysis

157 To obtain neurophysiologically realistic sources of neuronal activity, we applied complex-valued
158 independent component analysis in the frequency-domain (Fourier-ICA; (Hyvärinen et al.,
159 2010)) to MEG sensor's time series. The time series were divided into four-second epochs with
160 75 percent overlap and the epochs were Fourier transformed within the range of 4–24 Hz. A
161 complex-valued ICA using 64 PCA components was applied to the epochs (from first sessions
162 only), concatenated across subjects, which provided a group-level ICA un-mixing matrix. Note
163 that the effective dimension of the data was reduced to approximately 64 by SSS.

Component selection criteria

165 Often, several independent components in MEG reflect physiological activity that is unrelated to
166 neuronal activity of the brain (Jas et al., 2017). To exclude possible confounders, we applied
167 three criteria to select independent components. *First*, we included only components that had a
168 spectral peak within the range 8–16 Hz and the power of this peak was at least 50% larger than
169 the power in theta (4–7 Hz) or high-beta (17–24 Hz) bands. Before this comparison, we
170 equalized the spectral power over frequencies by subtracting the best fitting power-law function
171 from the power spectra. *Second*, we analysed the component's spatial maps and excluded those
172 components that had more than three blobs (i.e., continuous areas containing 5% of largest
173 values) in the spatial map. *Third*, we excluded the components if their maximum in spatial map
174 was located in the frontal or tempo-frontal areas. As a result, 38 components (out of 64) were
175 selected for further analysis. Generally speaking, brain sources are spatially localized and band-
176 pass, which leads to our formulation of the first two criteria, and the third criterion was included
177 to exclude eye artifacts.

Spectral features extraction

179 The individual subjects' spectral features were extracted in the following manner. The sensor
180 time series were divided into four-second epochs with 75 percent overlap and the epochs were
181 Fourier transformed within the range of 4–24 Hz. The group-level ICA un-mixing matrix was
182 applied to these epochs, and the amplitude spectra of frequency-domain independent components
183 were computed (Suppl. Fig. 1A). In order to increase robustness of the spectral approach, we
184 averaged the spectral amplitudes within four frequency bands: theta (4–7 Hz), alpha (8–12 Hz),
185 low-beta (13–16 Hz) and high-beta (17–24 Hz). The amplitude spectra averaged inside these four
186 frequency bands were then used as features for classification.

Connectivity features extraction

188 As an alternative to the spectral features, individual connectivity features were extracted as
189 follows. Again, the sensor time series were divided into four seconds epochs with 75 percent
190 overlap and the epochs were Fourier transformed within the range of 4–24 Hz. The group-level
191 ICA un-mixing matrix was applied to these epochs and inverse Fourier transform was computed

192 to reconstruct components' time series. The independent component time series were filtered in
193 four frequency bands: theta (4–7 Hz), alpha (8–12 Hz), low-beta (13–16 Hz) and high-beta (17–
194 24 Hz). In contrast to the spectral feature case, the Pearson correlation coefficients were
195 computed for each pair of the components (Suppl. Fig. 1B), separately for each frequency band.
196 The correlation coefficients between epochs of independent component time series were well
197 above zero (Suppl. Fig. 2). The connectivity matrices were then vectorised and used as features
198 for classification.

199 *Feature dimensionality reduction*

200 To further improve the robustness of classification, we reduced the dimensionality of the
201 spectral- and connectivity-based features by applying an algorithm described by Kauppi and
202 colleagues (Kauppi et al., 2013). The idea is to compute, for each epoch and component, the
203 most discriminating spectral or connectivity feature, and only use that in the classification. The
204 dimensionality of features were thus reduced as follows,

$$V_{i,j} = \sum_{t \in T1} F_{i,t,j} - \sum_{t \in T2} F_{i,t,j}$$

$$P_{i,t} = \sum_{j} F_{i,t,j} \cdot \frac{V_{i,j}}{\|V_{i,}\|}$$

205 where **F** denotes a tensor containing the spectral or connectivity features (whose dimensions are
206 either: components=38 *by* epochs *by* frequency_bands=4; or: component_pairs=703 *by* epochs
207 *by* frequency_bands=4, respectively). Here, *i* denotes component or connectivity pair index; T1
208 and T2 are indices of task 1 and task 2 in the training dataset, respectively; $\|\cdot\|$ denotes vector
209 norm operator; $V_{i,}$ means the vector consisting of all the $V_{i,j}$ for different *j*. The final result is
210 given in matrix **P** which contains the resulting feature vectors of the epochs, with dimensions:
211 components=38 *by* epochs; or component_pairs=703 *by* epochs, for spectral- or connectivity-
212 based classification, respectively.

213 *Classification methods: individual vs. group classification*

214 The spectral and connectivity features with reduced dimensionality were classified using the
215 linear Support Vector Machine (SVM) algorithm as implemented in scikit-learn (Pedregosa et
216 al., 2011). We used two scenarios to train and test the classifiers. In the first scenario "individual
217 classifier", we trained the classifier using individual data from the first session and tested the
218 classifier using data from the second session. In the second scenario "group classifier", we
219 trained the classifier using data from both sessions and all subjects except one "testing" subject,
220 and tested the classifier using the testing subject's data from the second session. The second
221 scenario is more challenging, essentially providing information on the generalizability of the
222 classifier across subjects (Jayaram et al., 2016; Kia et al., 2017).

223 *Real-time computation*

224 We tested the computational time for both feature extraction and classification algorithms to
225 ensure that our approaches suit real-time applications. The algorithms implemented in Python

226 were launched on a Linux based laptop (Intel Core i5-3570 @ 3.40 GHz, 8.00 GB RAM). The
227 average feature extraction time (±SD) for single epoch was 0.0118±0.0085 and 0.0385±0.0192
228 second for the spectral and connectivity approaches, respectively. The average classification time
229 using linear SVM was 0.0212±0.0042 and 0.1310±0.0086 seconds for the spectral and
230 connectivity approaches respectively. Thus, the computational time was negligibly small
231 compared to the inter-epoch interval of 0.5 second.

232 *Statistical analysis of classification accuracies*

233 To assess the statistical differences between the classification accuracies for different tasks or for
234 different feature sets, we applied the Wilcoxon rank sum test.

235 *Statistical analysis of classification coefficients*

236 To evaluate the contribution of different spectral and connectivity features to the resulting
237 classification accuracy, we performed a statistical analysis of the significance of the
238 classification coefficients. The coefficients were divided by their absolute sum and averaged
239 across subjects and then compared against zero mean using a two-sided z-test. For the spectral-
240 based approach, we reported both uncorrected ($p < 0.05$) and Bonferroni corrected classification
241 coefficients, while for the connectivity-based approach, we reported only Bonferroni corrected
242 classification coefficients, since there the problem of multiple testing was more serious.

243

244 **Results**

245 We applied the spectral and connectivity approaches to investigate whether and how it is
246 possible to discriminate (decode) between mindfulness meditation (MF), future planning (FP)
247 and reflection on anxious-inducing emotional pictures (EP) tasks. We then analysed the
248 classification coefficients to identify neuronal correlates (spatial maps and spectral profiles)
249 associated with the mental states during task performance.

250 *Classification accuracy*

251 We first computed the classification accuracies using spectral and connectivity approaches (Fig.
252 2).

253   --------------------------------

254   **Figure 2 about here**

255   --------------------------------

256 Fig. 2. Spectral- and connectivity-based classification accuracies averaged across subjects for
257 (A) individual and (B) group classifiers. MF_FP denotes mindfulness meditation vs. future
258 planning task, MF_EP denotes mindfulness meditation vs. reflection of anxious-inducing
259 emotional pictures task, and FP_EP denotes future planning task vs. reflection of anxious-
260 inducing emotional pictures task. Error bars represent SEM.

7

261 The spectral approach with individual classifier provided accuracies well above chance-level,
262 0.59±0.008 (MF vs. FP), 0.61±0.007 (MF vs. EP) and 0.55±0.005 (FP vs. EP). The accuracies
263 MF vs. FP and MF vs. EP were significantly larger ($p < 0.004$, individual classifier; $p < 0.01$,
264 group classifier) than the accuracy FP vs. EP, suggesting that FP and EP have similar neuronal
265 correlates. The accuracies for the group spectral-based classifier were relatively low, 0.55±0.003
266 (MF vs. FP), 0.54±0.003 (MF vs. EP) and 0.52±0.002 (FP vs. EP), showing that the classifier
267 had poor generalization over subjects.

268 The connectivity approach provided slightly higher accuracies compared to the spectral
269 approach, 0.62±0.009 (MF vs. FP), 0.62±0.009 (MF vs. EP) and 0.55±0.004 (FP vs. EP).
270 However, the accuracies were not significantly different ($p > 0.05$) between the spectral and
271 connectivity classifiers. The accuracies at the group level classifier were similar to those of the
272 spectral approach, 0.55±0.004 (MF vs. FP), 0.54±0.002 (MF vs. EP) and 0.53±0.002 (FP vs. EP).

273 We repeated the analysis by swapping training and testing sessions. There was no difference
274 between accuracies for the original and swapped sessions for the individual classifier, but the
275 difference became non-significant for the group classifier (Suppl. Fig. 3).

276 *Relationship between spectral- and connectivity-based accuracies*

277 To compare of the approaches further, we assessed the relationship (correlation) between
278 accuracies of spectral- and connectivity-based classifiers at individual subject's level (Fig. 3).
279 The results showed a significant correlation between spectral- and connectivity-based accuracies
280 only for two tasks, MF vs. FP ($r = 0.53$, $p < 0.008$) and MF vs. EP ($r = 0.60$, $p < 0.002$) for
281 individual classifier.

282 -------------------------------

283 **Figure 3 about here**

284 -------------------------------

285 Fig. 3. Scatter plots of individual subject's accuracies computed using spectral and connectivity
286 approaches for the following tasks, (A) mindfulness mediation vs. reflection on future planning
287 (MF_FP), (B) mindfulness mediation vs. reflection on anxiety-inducing emotional pictures
288 (MF_EP) and (C) reflection on future planning vs. reflection on anxiety-inducing emotional
289 pictures (FP_EP).

290 For the further analysis, we considered only results of the individual classifier and two tasks
291 (MF_FP and MF_EP).

292 *Spectral and connectivity projections*

293 We analysed the projection weights provided by the dimensionality reduction algorithm (see,
294 Materials and Methods), to evaluate the frequency-specific differences between the tasks.

295 The results showed that that largest difference between tasks was associated with alpha
296 frequency (Fig. 4). For the spectral classifier, the projection weights at alpha frequency were a
297 little larger compared to those of connectivity classifier. Surprisingly, there was a strong

8

298 variability of the projection weights for group spectral classifier for different tasks, in contrast to
299 individual spectral and connectivity classifiers.

300 --------------------------------

301 **Figure 4 about here**

302 --------------------------------

303 Fig. 4. Group level spectral and connectivity projections. Error bars represent SEM.

304 This result suggested that indeed, alpha frequency play an important role in discriminating
305 mindfulness and thought-inducing tasks.

306 *Classification coefficients of the spectral approach*

307 We analysed the SVM classification coefficients of spectral classifier to evaluate the impact of
308 different independent components and frequency bands on the accuracy. The coefficients obeyed
309 Gaussian distribution and we picked those coefficients whose absolute values were above the
310 chance-level corresponding to $p < 0.05$ (Fig. 5).

311 --------------------------------

312 **Figure 5 about here**

313 --------------------------------

314 Fig. 5. (A) Classification coefficients (absolute values) of spectral approach for the individual
315 classifier. The significant coefficients indicated by black ($p < 0.05$, uncorrected) and red ($p <$
316 0.05, Bonferroni corrected) arrows, respectively. (B) Spatial maps and spectral profiles of
317 independent components associated with significant coefficients. The grey curves indicate power
318 spectra with subtracted power-law fit.

319 There were a few independent components (all independent components are shown in Suppl.
320 Fig. 4A and 4B) associated with significantly larger classification coefficients. The components
321 were associated with both thought-inducing tasks, showing a slight increase in power spectra at
322 alpha frequency and located in the occipital (components 16, 20 and 30) or central areas
323 (component 11). After correcting for multiple testing, only one coefficient (component 30)
324 remained significant. Importantly, none of the significant weights was associated with
325 components characterised by strong (very clearly peaked) alpha oscillations, although several
326 such components were available for classification (see Suppl. Fig. 4A and 4B).

327 These results showed that rhythmic activity in occipital areas, but apparently not exclusively in
328 alpha frequency, makes the strongest contribution to the discrimination of mindfulness and
329 thought-inducing tasks.

330 To further elucidate the classification weights for individual subjects, we selected four largest
331 coefficients and associated components. The results showed that the components associated with
332 largest coefficients were highly individual (Suppl. Fig. 5), which make generalization of the
333 classifier coefficients over subjects impractical.

Classification coefficients of the connectivity approach

The connectivity approach provided similar classification accuracies to the spectral approach, although these approaches utilized different principles for feature extraction. Similarly to the spectral approach, the classification coefficients followed a Gaussian distribution. We applied a t-test and selected significant ($p < 0.05$, Bonferroni corrected) classification coefficients (Fig. 6).

Figure 6 about here

Fig. 6. (A) Significant classification coefficients representing connections (i.e., connectivity pairs), for individual classifier. (B) Node degree when considering only the significant connections shown in panel A. Degree of zero means that there are no significant connections. The significant components with node degree above one indicated by arrows. (C) Spatial maps and spectral profiles of independent components associated with component's node degree above one.

The results showed that multiple connections contribute to the classification accuracy (Fig. 6A). To identify the independent components that represented a hub (i.e., node with a high degree) and hence, more strongly influenced the classification accuracy, we analysed the node degrees of the components using only the significant connections (Fig. 6B). We selected the components with node degree above one, and further analysed them (Fig. 6C).

Similarly to the spectral approach, strongest connections were associated with the occipital and temporal components, some of which demonstrated a peak at alpha frequency. Only one component (component 17) was characterized by particularly prominent alpha oscillations (see Suppl. Fig. 4A and 4B for comparison), again suggesting that alpha oscillations may not be strongly related to mindfulness states.

These results demonstrated a considerable variety of spatial maps and spectral patterns, which can underlie the difference in mindfulness and thought-provoking tasks.

To evaluate the contribution of high node degree components in individual subjects, we selected four components with highest node degree for each subject. The results showed that the high node degree components were highly individual (Suppl. Fig. 6), and similarly to the spectral-based classification, generalization over the subjects seems impractical.

All components classification

As noted in the Materials and Methods section, we excluded independent components that seem to be strongly contaminated by non-brain physiological artifacts. However, it is interesting to assess the impact such components would have on the classification. To accomplish this, we selected all the 64 independent components and applied the spectral- and connectivity-based classification approaches (Fig. 7).

10

371   -------------------------------

372   **Figure 7 about here**

373   -------------------------------

374 Fig. 7. Classification accuracies for (A) spectral and (B) connectivity approaches using 38 (solid
375 bars) and 64 (dashed bars) components for individual and group classifiers.

376 We observed no differences in the accuracy for 38 and 64 independent components for the
377 individual spectral and connectivity classifiers, as well as for the group connectivity classifier
378 (Fig. 7). However, there were large differences in the accuracy for the group spectral classifier in
379 MF vs. FP ($p < 0.001$) and MF vs. EP ($p < 0.03$).

380 To clarify the difference, we analysed the classification coefficients of the group spectral
381 classifier (Fig. 8).

382   -------------------------------

383   **Figure 8 about here**

384   -------------------------------

385 Fig. 8. (A) The coefficients of the group spectral classifier for 64 independent components. The
386 significant coefficients indicated by black ($p < 0.05$, uncorrected) and red ($p < 0.05$, Bonferroni
387 corrected) arrows, respectively. (B) The spatial maps and spectral profiles associated with the
388 significant coefficients.

389 The results clearly showed that when artifacts were not removed, the classifier picked the
390 components that were mainly associated with physiological artifacts such as eye-blinks
391 (component 6 and 18), cardiac activity (component 52), instrumental noise or other physiological
392 artifacts (20, 50, 56). On the other hand, the possibly sensory-motor component (15) may have
393 been erroneously excluded from the main analysis. After correcting for multiple testing, three
394 coefficients (components 18, 50 and 52) remained significant.

395 In this case, the higher accuracy of the group spectral classifier likely to be related to the fact that
396 the artifacts were highly consistent across subjects (Smith and Nichols, 2018), and thus provided
397 a better basis for generalizing to new subjects.

398 *Individual and group ICA*

399 To evaluate the impact of ICA on classification accuracy, we recomputed the accuracies using
400 spectral- and connectivity-based classifiers for individual and group ICA weights. Because the
401 spectral profiles and spatial maps of individual independent components strongly varied across
402 subjects, we did not apply the component selection criteria (see, *Materials and Methods*) and
403 computed the classification accuracies for all 64 components (Fig. 9). There were no significant
404 differences in the accuracies for individual and group ICA. This means that ICA spatial filters
405 can be precomputed in advance and the classification approach can be operated in real time.

406

407   -------------------------------

408   **Figure 9 about here**

409   -------------------------------

410   Fig. 9. Classification accuracies for the individual and group ICA weights using (A) spectral and
411   (B) connectivity approaches.

412

413   **Discussion**

414   In this study, we developed spectral- and connectivity-based classification approaches and
415   showed that the mental states underlying mindfulness and thought-provoking tasks can be
416   discriminated using MEG recordings and machine learning approaches.

417   We observed a variety of spatial and spectral patterns that contribute to discriminating
418   mindfulness meditation, suggesting that several neuronal mechanisms may underlie mindfulness
419   state. While the results in Fig. 4 indicate that the alpha frequency band is the most important,
420   they also show the major contribution of other bands for classification. Moreover, our detailed
421   analysis showed that none of the strongest classification weights was associated with
422   components characterised by particularly strong alpha oscillations. Indeed, among many
423   components with a noticeable peak at the alpha frequency, the components with the most
424   pronounced peaks in alpha frequency (clearly oscillatory components) did not show any
425   significant contribution to the discrimination. This seems to refute the conventional view on
426   mindfulness meditation where the mindfulness state is tightly related to alpha frequency
427   oscillations (Kerr et al., 2013). However, one caveat is that we used rather inexperienced
428   meditators, and the situation might be different in the case of more experienced meditators.

429   In our results, spectral and connectivity features gave similar classification accuracies, which
430   raises the question of whether they contain the same information. This does not seem to be so
431   based on comparisons of the most important sources in Figures 5 and 6, and so it would seem
432   that the similar classification accuracies may be only a coincidence. However, since our
433   connectivity measures used zero lag, some overlapping information is likely to be present.

434   We visualized the spatial weights enabling classification between mindfulness and the tasks
435   simulating wandering thoughts. It should be noted that the connection between these classifier
436   weights and the neural correlates is not straight-forward. Interpretation of the weights can lead to
437   wrong conclusions regarding the origin of neural signals of interest, since significant nonzero
438   weights may also be associated with task-irrelevant signals (Haufe et al., 2014). However, from a
439   neurofeedback viewpoint, the classifier weights reported here show which brain areas should be
440   measured, e.g. in a case of building a portable EEG cap with a small number of sensors.

441   Considering that the task-relevant frequencies and brain regions may not be simply linked to the
442   classification weights, there have been a few attempts to clarify the neuronal basis of
443   mindfulness meditation. Gil and colleagues (Navarro Gil et al., 2018) showed that an EEG
444   neurofeedback that aims at increasing power at the alpha frequency, improves mindfulness

outcome, and thus, may be effective for increasing mindfulness in healthy individuals. Unfortunately, the neurofeedback signal in this study was derived by averaging a set of occipital-parietal electrodes, which makes difficult to assess the location of underlying sources. Another EEG study (van Lutterveld et al., 2017) overcame such limitation by deriving the neurofeedback signal in a source space. The neurofeedback was provided based on gamma-band activity (40–57 Hz) from the posterior parietal cortex. The subjects were able to volitionally control the neurofeedback signal in the direction associated with effortless awareness by practicing effortless awareness meditation. Hence, these two studies suggested that not only alpha but also other frequencies are associated with mindfulness meditation, and parietal cortex may have a key role in mindfulness.

We observed relatively low classification accuracy in discriminating between future planning and reflection on anxiousness-inducing emotional pictures tasks, which suggests similarity of the rhythmic neuronal activity as captured by MEG during these tasks. Although these tasks are behaviourally quite different, and likely to be different in terms of amplitudes of the evoked responses in an affective picture paradigm (Olofsson et al., 2008), they may be similar in terms of task-nonspecific cortical processes related to attentional states. Consequently, our analysis, focusing on ongoing brain activity, may not be sensitive to this difference.

The overall classification accuracy in this study was nearly sixty percent, which is relatively low for a neurofeedback system. However, accuracies for a few participants were around seventy percent or more, which may allow a significant improvement in mindfulness meditation. Moreover, this relatively low accuracy may be explained by the fact that the subjects did not have previous experience in mindfulness meditation. Possibly, the neurofeedback might work much better after subjects gain more experience. Generalization over subjects was even more difficult, presumably due to the large individual differences and the methods are more likely to work when a large amount of data can be collected from each single subject. However, it should be noted that advanced multi-task classification methods might be able to generalize better by either finding some structure in data that is invariant across subjects or finding some structure in the decision rules between different subjects (Jayaram et al., 2016; Kia et al., 2017). Furthermore, combining brain measurements with psychophysiological measurements (for instance, heart-rate variability (Nesvold et al., 2012)) and other modalities might be useful to obtain practically useful classification performance in future research.

Acknowledgements

References

Andrews-Hanna, J.R., Smallwood, J., Spreng, R.N., 2014. The default network and self-generated thought: component processes, dynamic control, and clinical relevance. Ann. N. Y. Acad. Sci. 1316,

485   29–52. https://doi.org/10.1111/nyas.12360

486   Baldwin, C.L., Roberts, D.M., Barragan, D., Lee, J.D., Lerner, N., Higgins, J.S., 2017. Detecting and
487   Quantifying Mind Wandering during Simulated Driving. Front. Hum. Neurosci. 11, 406.
488   https://doi.org/10.3389/fnhum.2017.00406

489   Blankertz, B., Lemm, S., Treder, M., Haufe, S., Müller, K.-R., 2011. Single-trial analysis and
490   classification of ERP components — A tutorial. Neuroimage 56, 814–825.
491   https://doi.org/10.1016/j.neuroimage.2010.06.048

492   Braboszcz, C., Delorme, A., 2011. Lost in thoughts: neural markers of low alertness during mind
493   wandering. Neuroimage 54, 3040–7. https://doi.org/10.1016/j.neuroimage.2010.10.008

494   Brookes, M.J., Woolrich, M., Luckhoo, H., Price, D., Hale, J.R., Stephenson, M.C., Barnes, G.R., Smith,
495   S.M., Morris, P.G., 2011. Investigating the electrophysiological basis of resting state networks using
496   magnetoencephalography. Proc. Natl. Acad. Sci. U. S. A. 108, 16783–8.
497   https://doi.org/10.1073/pnas.1112685108

498   Christoff, K., Gordon, A.M., Smallwood, J., Smith, R., Schooler, J.W., 2009. Experience sampling during
499   fMRI reveals default network and executive system contributions to mind wandering. Proc. Natl.
500   Acad. Sci. 106, 8719–8724. https://doi.org/10.1073/pnas.0900234106

501   Haufe, S., Meinecke, F., Görgen, K., Dähne, S., Haynes, J.-D., Blankertz, B., Bießmann, F., 2014. On the
502   interpretation of weight vectors of linear models in multivariate neuroimaging. Neuroimage 87, 96–
503   110. https://doi.org/10.1016/j.neuroimage.2013.10.067

504   Hyvärinen, A., Ramkumar, P., Parkkonen, L., Hari, R., 2010. Independent component analysis of short-
505   time Fourier transforms for spontaneous EEG/MEG analysis. Neuroimage 49, 257–271.
506   https://doi.org/10.1016/j.neuroimage.2009.08.028

507   Jas, M., Engemann, D.A., Bekhti, Y., Raimondo, F., Gramfort, A., 2017. Autoreject: Automated artifact
508   rejection for MEG and EEG data. Neuroimage 159, 417–429.
509   https://doi.org/10.1016/j.neuroimage.2017.06.030

510   Jayaram, V., Alamgir, M., Altun, Y., Scholkopf, B., Grosse-Wentrup, M., 2016. Transfer Learning in
511   Brain-Computer Interfaces Abstract\uFFFDThe performance of brain-computer interfaces (BCIs)
512   improves with the amount of avail. IEEE Comput. Intell. Mag. 11, 20–31.
513   https://doi.org/10.1109/MCI.2015.2501545

514   Kauppi, J.-P., Parkkonen, L., Hari, R., Hyvärinen, A., 2013. Decoding magnetoencephalographic
515   rhythmic activity using spectrospatial information. Neuroimage 83, 921–936.
516   https://doi.org/10.1016/j.neuroimage.2013.07.026

517   Kerr, C.E., Sacchet, M.D., Lazar, S.W., Moore, C.I., Jones, S.R., 2013. Mindfulness starts with the body:
518   somatosensory attention and top-down modulation of cortical alpha rhythms in mindfulness
519   meditation. Front. Hum. Neurosci. 7, 12. https://doi.org/10.3389/fnhum.2013.00012

520   Kia, S.M., Pedregosa, F., Blumenthal, A., Passerini, A., 2017. Group-level spatio-temporal pattern
521   recovery in MEG decoding using multi-task joint feature learning. J. Neurosci. Methods 285, 97–
522   108. https://doi.org/10.1016/j.jneumeth.2017.05.004

523   Kucyi, A., 2017. Just a thought: How mind-wandering is represented in dynamic brain connectivity.
524   Neuroimage. https://doi.org/10.1016/j.neuroimage.2017.07.001

525   Lemm, S., Blankertz, B., Dickhaus, T., Müller, K.-R., 2011. Introduction to machine learning for brain
526   imaging. Neuroimage 56, 387–399. https://doi.org/10.1016/j.neuroimage.2010.11.004

527   Lotte, F., Congedo, M., Lécuyer, A., Lamarche, F., Arnaldi, B., 2007. A review of classification
528   algorithms for EEG-based brain–computer interfaces. J. Neural Eng. 4, R1–R13.
529   https://doi.org/10.1088/1741-2560/4/2/R01

530   Navarro Gil, M., Escolano Marco, C., Montero-Marín, J., Minguez Zafra, J., Shonin, E., García Campayo,
531   J., 2018. Efficacy of Neurofeedback on the Increase of Mindfulness-Related Capacities in Healthy
532   Individuals: a Controlled Trial. Mindfulness (N. Y). 9, 303–311. https://doi.org/10.1007/s12671-
533   017-0775-1

534   Nesvold, A., Fagerland, M.W., Davanger, S., Ellingsen, Ø., Solberg, E.E., Holen, A., Sevre, K., Atar, D.,
535   2012. Increased heart rate variability during nondirective meditation. Eur. J. Prev. Cardiol. 19, 773–
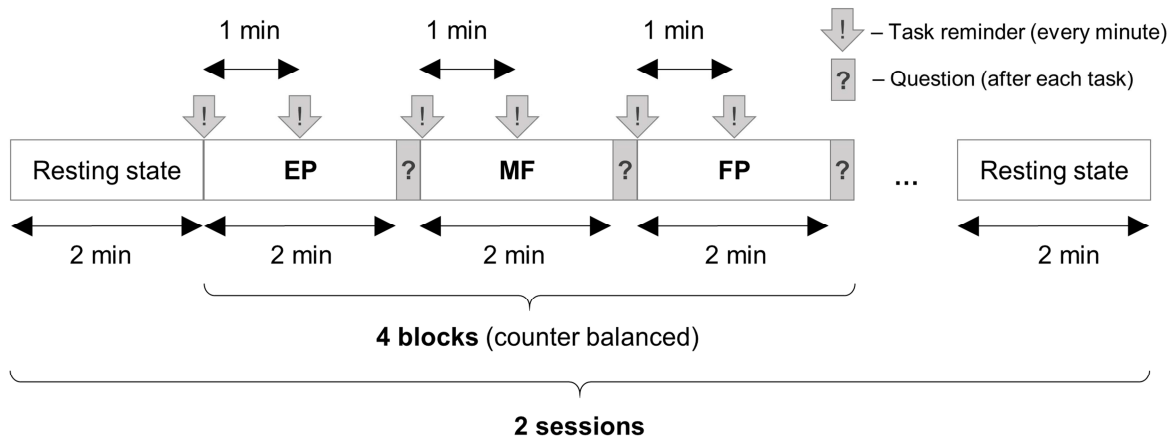
536   780. https://doi.org/10.1177/1741826711414625
537 Olofsson, J.K., Nordin, S., Sequeira, H., Polich, J., 2008. Affective picture processing: an integrative
538   review of ERP findings. Biol. Psychol. 77, 247–65. https://doi.org/10.1016/j.biopsycho.2007.11.006
539 Pedregosa, F., Varoquaux, G., Gramfort, A., Michel, C., Thirion, B., Grisel, O., Blondel, M.,
540   Prettenhoffer, P., Weiss, R., Dubourg, V., Vanderplas, J., Passos, A., Cournapeau, D., 2011. Scikit-
541   learn: Machine learning in Python. J. Mach. Learn. Res. https://doi.org/10.1007/s13398-014-0173-
542   7.2
543 Ros, T., Théberge, J., Frewen, P.A., Kluetsch, R., Densmore, M., Calhoun, V.D., Lanius, R.A., 2013.
544   Mind over chatter: plastic up-regulation of the fMRI salience network directly after EEG
545   neurofeedback. Neuroimage 65, 324–35. https://doi.org/10.1016/j.neuroimage.2012.09.046
546 Scheeringa, R., Fries, P., Petersson, K.-M., Oostenveld, R., Grothe, I., Norris, D.G., Hagoort, P.,
547   Bastiaansen, M.C.M., 2011. Neuronal Dynamics Underlying High- and Low-Frequency EEG
548   Oscillations Contribute Independently to the Human BOLD Signal. Neuron 69, 572–583.
549   https://doi.org/10.1016/J.NEURON.2010.11.044
550 Schmidt, E.A., Schrauf, M., Simon, M., Fritzsche, M., Buchner, A., Kincses, W.E., 2009. Drivers'
551   misjudgement of vigilance state during prolonged monotonous daytime driving. Accid. Anal. Prev.
552   41, 1087–1093. https://doi.org/10.1016/j.aap.2009.06.007
553 Smith, S.M., Nichols, T.E., 2018. Statistical Challenges in "Big Data" Human Neuroimaging. Neuron 97,
554   263–268. https://doi.org/10.1016/j.neuron.2017.12.018
555 Tang, Y.-Y., Posner, M.I., Rothbart, M.K., 2014. Meditation improves self-regulation over the life span.
556   Ann. N. Y. Acad. Sci. 1307, 104–111. https://doi.org/10.1111/nyas.12227
557 Taulu, S., Kajola, M., Simola, J., 2004. Suppression of interference and artifacts by the Signal Space
558   Separation Method. Brain Topogr. 16, 269–75.
559 van Lutterveld, R., Houlihan, S.D., Pal, P., Sacchet, M.D., McFarlane-Blake, C., Patel, P.R., Sullivan,
560   J.S., Ossadtchi, A., Druker, S., Bauer, C., Brewer, J.A., 2017. Source-space EEG neurofeedback
561   links subjective experience with brain activity during effortless awareness meditation. Neuroimage
562   151, 117–127. https://doi.org/10.1016/j.neuroimage.2016.02.047
563 Wolpaw J., Birbaumer N., McFarland D., Pfurtscheller G., Vaughan T., 2002. Brain-computer interfaces
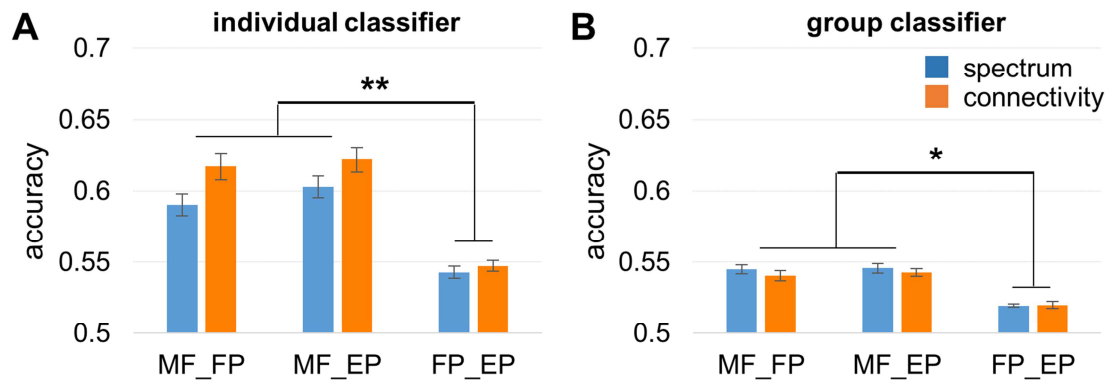564   for communication and control. Clin. Neurophysiol.
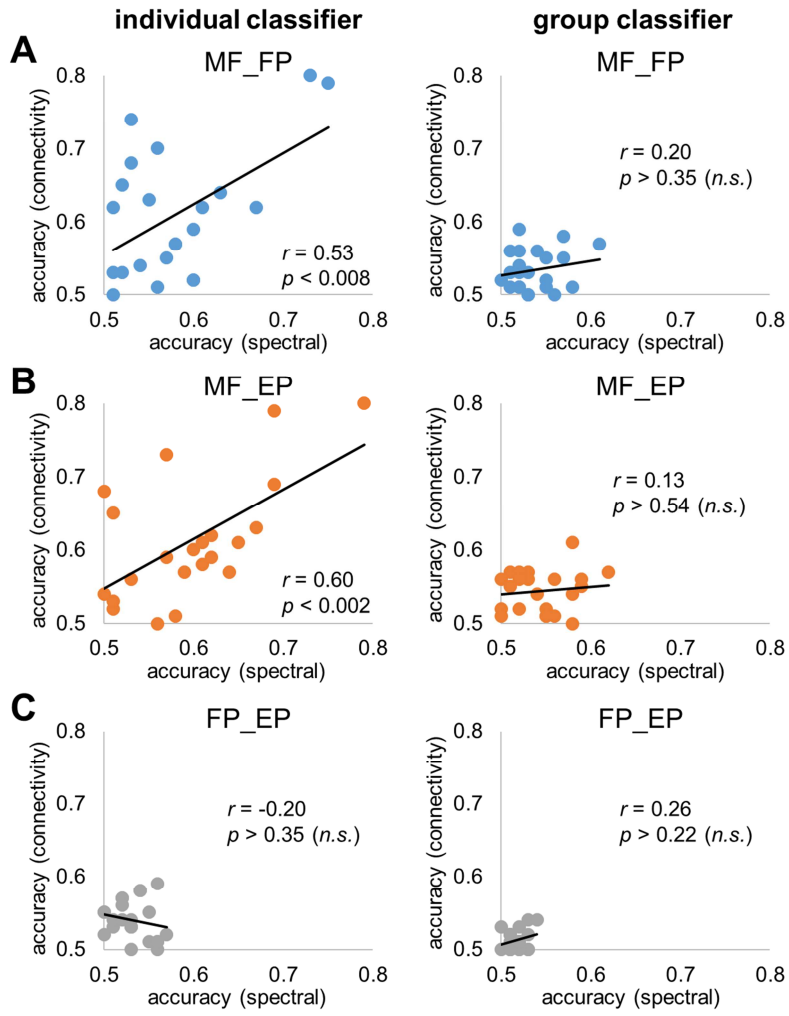
565
566
567 **Supplementary figure legends**

568 Suppl. Fig. 1. Schematic representation of the feature extraction in (A) spectral and (B)
569 connectivity approaches.

570 Suppl. Fig. 2. Distribution of the correlation coefficients for different frequency bands in
571 connectivity approach.

572 Suppl. Fig. 3. Classification accuracy for swapped training and testing sessions.

573 Suppl. Fig. 4A. The spatial maps and spectral profiles of group-level independent components (1
574 to 20).

575 Suppl. Fig. 4B. The spatial maps and spectral profiles of group-level independent components
576 (21 to 38).

577 Suppl. Fig. 5. (A, B) Four largest individual classification coefficients associated with
578 independent components for spectral classifier in (A) MF_FP and (B) MF_EP tasks.
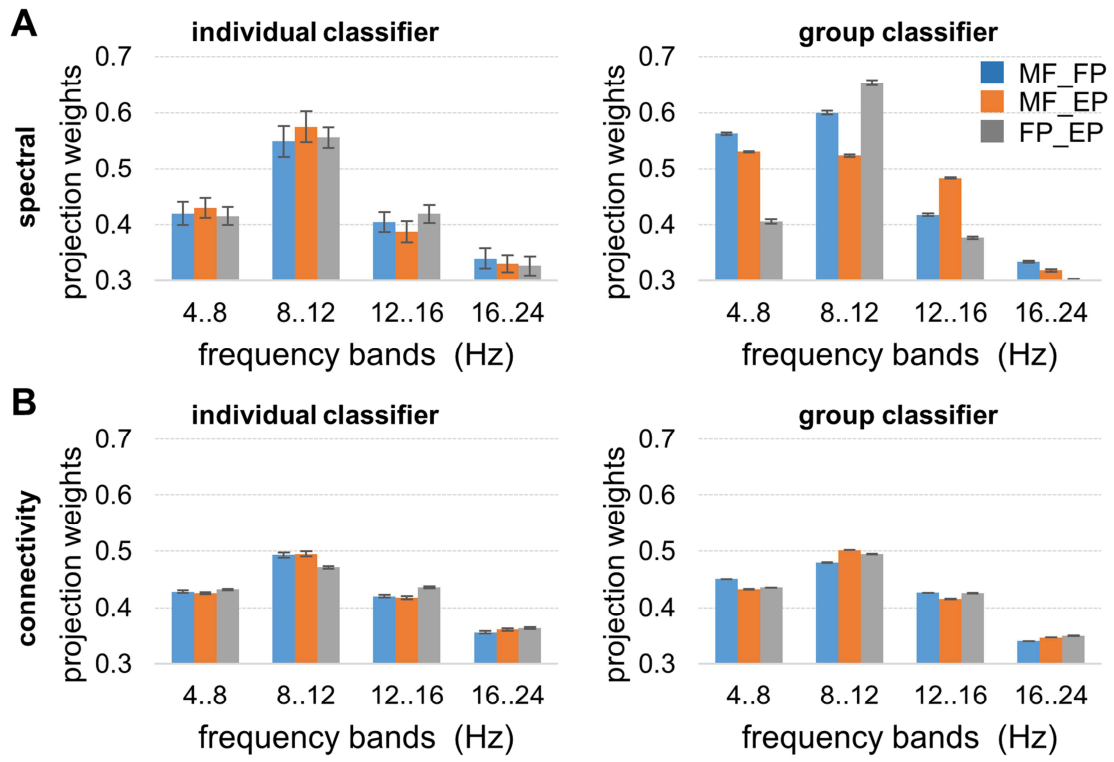
579 Suppl. Fig. 6. (A, B) Four individual independent components with highest degree node for
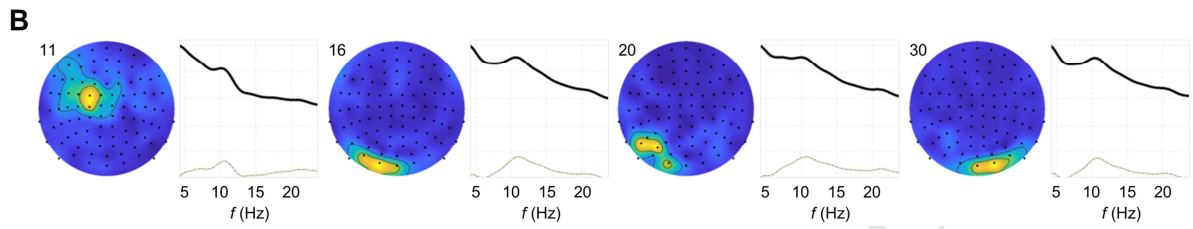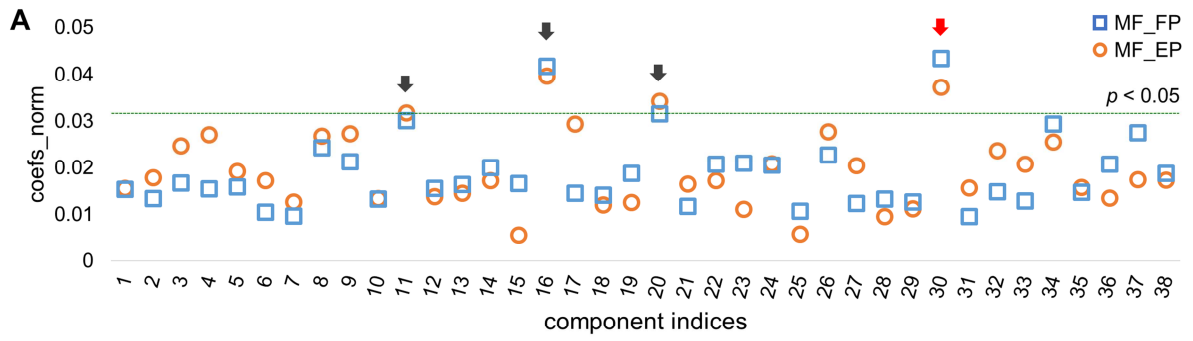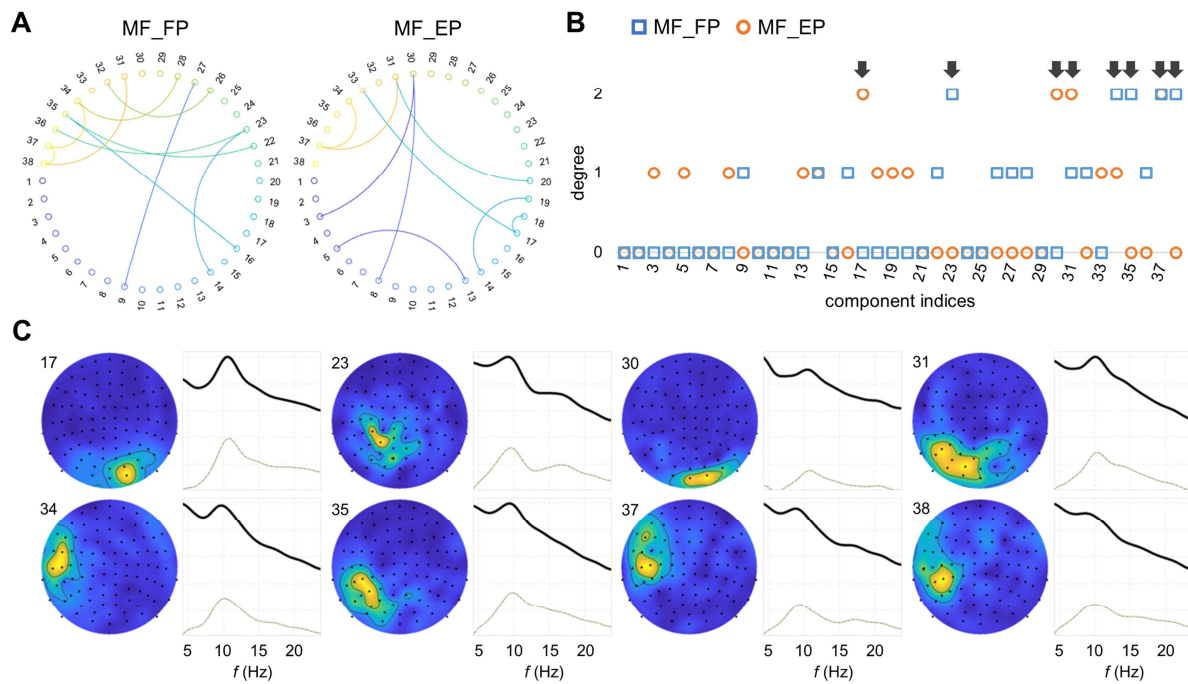580 connectivity classifier in (A) MF_FP and (B) MF_EP tasks.

individual classifier   **group classifier**

A   MF_FP
$r = 0.53$
$p < 0.008$

MF_FP
$r = 0.20$
$p > 0.35$ (*n.s.*)

B   MF_EP
$r = 0.60$
$p < 0.002$

MF_EP
$r = 0.13$
$p > 0.54$ (*n.s.*)

C   FP_EP
$r = -0.20$
$p > 0.35$ (*n.s.*)

FP_EP
$r = 0.26$
$p > 0.22$ (*n.s.*)

A

spectral classifier

B

connectivity classifier